NORMALIZED PROJECTED RED & SWIR (NPRS): A NEW VEGETATION INDEX FOR FOREST HEALTH ESTIMATION AND ITS APPLICATION ON SPRUCE BARK BEETLE ATTACK DETETION

Langning Huo, Eva Lindberg and Henrik Persson

Department of Forest Resource Management,
Swedish University of Agricultural Sciences, Umeå, Sweden

ABSTRACT

Due to the ongoing global warming, European spruce bark beetles has become a serious threat to the spruce forests in Europe and caused serious environmental and economic issues. This study proposes a new vegetation index, Normalized Projected Red & SWIR (NPRS), for detection of spruce bark beetle attacks. 29 healthy and 24 bark beetle attacked plots in southern Sweden were used for evaluating the classification accuracy using NPRS at early-, intermediate- and late-stage attacks. The obtained kappa coefficients were 0.73, 0.80 and 0.88, respectively. It was concluded that the NPRS is a feasible method for continuous bark beetle mapping over large areas.

***Index Terms*—** bark beetle attacks, vegetation index, early detection

1. INTRODUCTION

The European spruce bark beetle (*Ips typographus* [L.]) is one of the insects in coniferous forests causing the largest economical damage in Europe [1, 2]. Furthermore, it is a serious threat to the forest ecosystems and sustainable forest managements. One efficient strategy for damage control is monitoring of the forests using remote sensing data, to detect attacks and possibly remove stems with larva still inside before the bark beetles swarm for the next generation. The early stage of the attacks, known as "green attacks" [3–6], is the most important time for forest management, but also the most difficult period for detection because there is almost no color change in the tree crowns. Yet, optical remote sensing images provide additional wavelengths outside the visual spectra. These have potential to be used for mapping the change under early-stage attacks.

Non-conclusive results have been presented in earlier studies regarding how the red edge and near inferred (NIR) bands behaved. In most studies, common indices like Normalized Difference Vegetation Index (NDVI) and Normalized Difference Water Index (NDWI) have been used and recommended [7, 8]. Both these indices are based on the NIR band. However, Klouček et al. [9] concluded that the performance of indices based on the NIR band was lower than those based on the red band. Due to the inconsistent results in the studies based on the NIR band, additional alternatives for robust bark beetle detection should be explored.

This study proposes a new vegetation index, NPRS, using the red and SWIR bands from the Sentinel-2 satellite, to identify attacks in early, intermediate and late stages. Classification accuracy and estimation maps are presented as the evaluation.

2. MATERIALS

The study area in Remningstorp, Västra Götaland, Sweden (58°27′18.35″N, 13°39′8.03″E), covers an area of 1,602 hectares. The forest in the area is mainly managed Norway spruce (*Picea abies L. Karst.*) for wood production. In 2019, according to the swarm monitoring station records from SODAR, a forest owners' association, the first and second generations of bark beetles started swarming and attacking trees in week 15 (April 8 to 15) and week 31 (July 29 to August 4), respectively. Most of the offspring from the second generation remained in the bark at least until early September.

A field inventory was conducted in June 2019. Sample plots were placed in mature, spruce-dominated stands and the status of trees with DBH$\geqslant$10 cm were recorded. Bark beetle attacks were revealed through resin flows, beetle crumbs/flour and traces of woodpeckers searching for insects. Totally 53 sample plots with 15 m radius were used to present the performance of NPRS on spruce bark beetle attack detection, of which 24 plots had ongoing bark beetle attacks and 29 were healthy plots. The proportion of attacked trees in each plot ranged from 14% to 59%, with an average of 31%. Attacked and healthy plots had similar distributions of stem density and biomass.

Optical images were obtained from Sentinel-2, a European wide-swath, high-resolution, multi-spectral imaging satellite mission. Three cloud-free L2A images for 2019/04/07, 2019/07/26 and 2019/10/07 were acquired. The average pixel values for each plot were extracted for the red band (665 nm and 10 m resolution) and the SWIR band (2202 nm and 20 m resolution).

3. METHODS

An index was created based on the linear relation between the red and the SWIR bands, as

$$\mathrm{SWIR} = \mathrm{k} \times \mathrm{Red} + \mathrm{b} \quad (1)$$

where k and b are the slope and intercept of the linear regression between the red and the SWIR band.

All images in our dataset showed a similar linear relation but with slightly different values of k and b (Figure 1). Attacked plots showed larger pixel values in the red and SWIR bands, distributed further away from the intercept along the regression line (Figure 1), when compared with the healthy plots. The Projected Red SWIR (PRS, Figure 1d) could be calculated using Equation (2) as

$$\mathrm{PRS} = \frac{k^2 \times SWIR + k \times Red + b}{\sqrt{k^2 \times (1 + k^2)}} \quad (2)$$

Since only one PRS value was needed as the threshold to identify attacks in this application, k and b were generalized to be 2 and 0 to simplify the calculation of PRS. This agrees with the suggestion proposed by Kaufman et al. [10], who used a large variety of land types. The PRS was therefore simplified to Equation (3) as

$$\mathrm{PRS} = \frac{Red + 2 \times SWIR}{\sqrt{5}} \quad (3)$$

The PRS was then normalized to 0 – 1 to attain a continuous distribution of attacked probabilities and with uniform thresholds for attack degree classification. The NPRS could finally be calculated as

$$\mathrm{NPRS} = \frac{PRS - PRS'_{min}}{PRS'_{max} - PRS'_{min}} \quad (4)$$

where PRS'_{max} and PRS'_{min} are the max and min values of the PRS from the spruce stands in the corresponding image. By using these values instead of the actual range obtained from the images, the extremes from other land types, such as clear-cut areas, were removed. The normalization made the NPRS more sensitive to the subtle optical change caused by bark beetle attacks, while clear-cut areas could still be detected by NPRS values close to 1. In this study, the range was derived based on pixel values from 14 spruce stands with closed canopy (PRS'). The 99% and 1% percentiles of their PRS values were used as PRS'_{max} and PRS'_{min}.

For detection of attacks, the NPRS index was calculated for the 53 plots. We used 0.5 as the threshold to classify the plots into healthy or attacked. The classification error was used as the evaluation of the NPRS performance.

A map of the bark beetle attacks was estimated for the selected forest stands in the entire satellite scene of the study area. The stands were selected to contain spruces comprising more than 80% of the stem volume. Spruce stands younger than 30 years were excluded since bark beetles primarily attack mature spruces. NPRS was calculated on 10 m reslution pixels using the image from 2019/04/07.

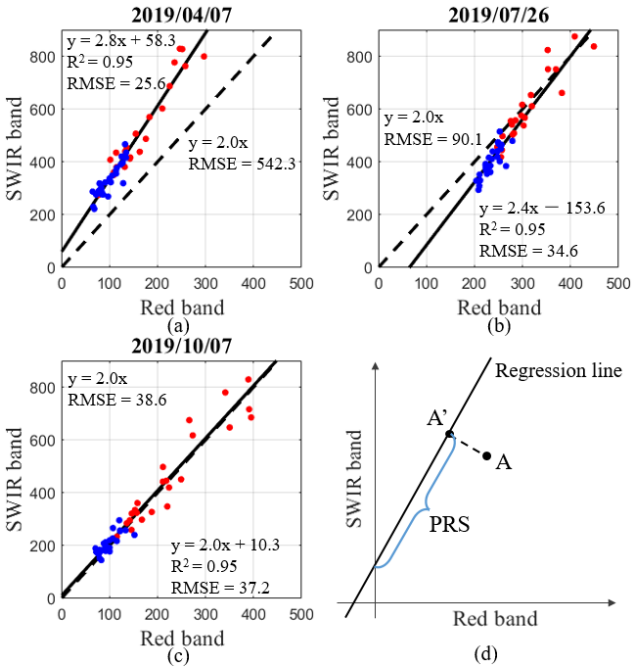

Figure 1. Pixel values from the red and SWIR bands for healthy (blue) and attacked (red) pixels. (a - c) images from 2019/04/07, 2019/07/26 and 2019/10/07. (d) The PRS of point A projected on the regression line.

4. RESULTS

The classification of healthy and attacked plots resulted in the kappa values 0.73, 0.80 and 0.88, for the three proceeding images, corresponding to early-, intermediate- and late-stage attacks. The estimation map with continuous NPRS values representing the attack probabilities are illustrated in Figure 2 (only part of the full map in order to show more details).

Table 1. Confusion matrix of the predictions at different attack stages. Class A for attacked plots, and Class H for healthy plots.

		Field inventory					
		Apr. 7		Jul. 26		Oct. 7	
Prediction	Class	A	H	A	H	A	H
	A	21	4	21	2	21	0
	H	3	25	3	27	3	29
	Kappa	0.73		0.80		0.88	

*A for attacked plots, H for healthy plots.

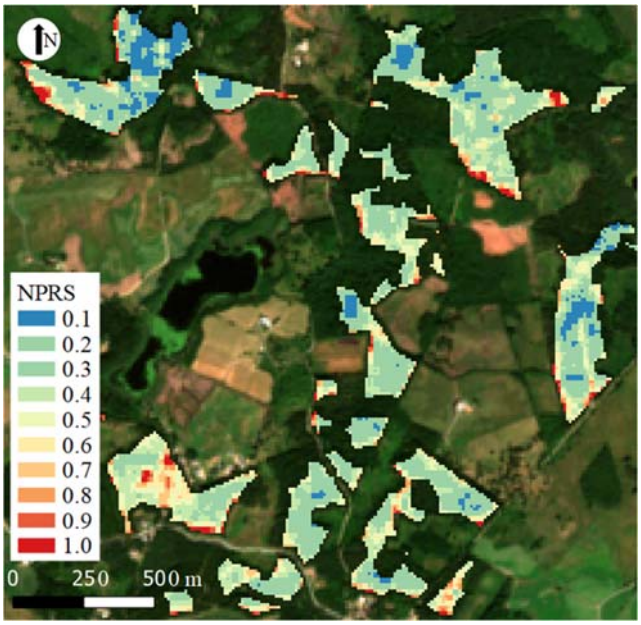

Figure 2. NPRS map for spruce stands from a subpart of the study area.

5. DISCUSSION

Bark beetle attacked forests showed significant increases of the red and the SWIR bands. Similar changes have been identified also in other studies [9, 10], and they appear to be related to the biochemical reaction due to the bark beetle attacks. Abdullah et al. [11] observed a clear distinction of foliar chlorophyll, leaf water content and stomatal conductance between leaves from healthy trees and trees attacked by bark beetles. Reductions in chlorophyll has been shown to decrease the spectral absorptance in the visible region, resulting in relatively higher reflectance, especially in the red band [12]. During the attacks, not only the larval feeding caused phloem girdling [13], but also the beetle-associated blue-stain fungi may dry the tissue and induce tracheid aspiration or vascular plugging [14]. Such changes in the water content would be sensed by the SWIR band [15].

The bark beetle index using the red and the SWIR bands proposed in this study is a combination which has been rarely used earlier [16]. This index was based on the linear relationship between the two bands. Such relations have been proposed more than twenty years ago [17], and they have been used in an aerosol free vegetation index when replacing the red or blue bands by the SWIR band (1.6 and 2.1 μm) [18]. In the latter study, the scatter plot of the red and the SWIR bands from different landscape pixels also showed that the pixel values distributed along the regression line, with pixels containing smaller proportions of forests scattered at further distance from the origin of coordinates. The index proposed in this study extends the work from previous studies and furthermore confirm their findings. When approximating the parameters k and b in the linear regression with 2 and 0 instead of using the actual values derived from the specific date, a small bias was introduced to the PRS index. Nevertheless, the classification accuracy illustrated that the simplified calculation was still sufficiently robust for spruce bark beetle detection.

For practical use, the PRS might also be affected by stand properties such as age, stem density, canopy density, species composition and biomass. Thus, it is recommended to use it on homogeneous spruce stands and normalized to NPRS using thresholds based on homogeneous spruce stands. In addition, weak and stressed trees also have high probabilities to be discriminated by NPRS based on the similar biochemical reaction. Different studies have illustrated the relationship between probability of an attack and soil nutrients [19], water supply [20] and topography [21]. Weakness caused by such factors would also be sensed from the tree crowns by optical images at early stage attacks or even describing the potential of successful attacks.

6. CONCLUSION

This study proposed a new vegetation index, NPRS, which can be used for identifying bark beetle attacked forest. NPRS was calculated from the red and SWIR bands based on their linear relation, and they were verified on 24 attacked and 29 healthy plots in southern Sweden. Sentinel-2 images from 2019/04/07, 2019/07/06 and 2019/10/07, were used for the classifications, resulting in the kappa coefficients 0.73, 0.80 and 0.88. Maps with continuous NPRS values as the attack probabilities were presented as a demonstration of practical use on spruce forests.

Further studies could be conducted using denser time-series of images, larger areas and more diversified forest types as reproducibility tests for the proposed NPRS index. We may also propose a hypothesis that NPRS could be used for detection of other forest insects, which are damaging barks and induce tracheid aspiration or vascular plugging. Such a hypothesis could be studied in the future for various forest damages and diseases. Similar studies on an individual tree level is also an option to test the potential improvement of detection accuracy.

7. REFERENCES

[1] P. H. W. Biedermann *et al.,* "Bark Beetle Population Dynamics in the Anthropocene: Challenges and Solutions," (eng), *Trends in ecology & evolution*, vol. 34, no. 10, pp. 914–924, 2019.

[2] M.-J. Schelhaas, G.-J. Nabuurs, and A. Schuck, "Natural disturbances in the European forests in the 19th and 20th centuries," *Global Change Biol*, vol. 9, no. 11, pp. 1620–1633, 2003.

[3] M. Hais *et al.,* "Landsat Imagery Spectral Trajectories—Important Variables for Spatially Predicting the Risks of Bark Beetle Disturbance," *Remote Sensing*, vol. 8, no. 8, p. 687, 2016.

[4] C.-y. Huang, W. R.L. Anderegg, and G. P. Asner, “Remote sensing of forest die-off in the Anthropocene: From plant ecophysiology to canopy structure,” *Remote Sensing of Environment*, vol. 231, p. 111233, 2019.

[5] J. C. White, N. C. Coops, T. Hilker, M. A. Wulder, and A. L. Carroll, “Detecting mountain pine beetle red attack damage with EO‐1 Hyperion moisture indices,” *International Journal of Remote Sensing*, vol. 28, no. 10, pp. 2111–2121, 2007.

[6] M. A. Wulder, C. C. Dymond, J. C. White, D. G. Leckie, and A. L. Carroll, “Surveying mountain pine beetle damage of forests: A review of remote sensing opportunities,” *Forest Ecology and Management*, vol. 221, no. 1-3, pp. 27–41, 2006.

[7] H. Abdullah, A. K. Skidmore, R. Darvishzadeh, and M. Heurich, “Sentinel‐2 accurately maps green‐attack stage of European spruce bark beetle (Ips typographus L.) compared with Landsat‐8,” *Remote Sens Ecol Conserv*, vol. 5, no. 1, pp. 87–106, 2019.

[8] S. Ortiz, J. Breidenbach, and G. Kändler, “Early Detection of Bark Beetle Green Attack Using TerraSAR-X and RapidEye Data,” *Remote Sensing*, vol. 5, no. 4, pp. 1912–1931, 2013.

[9] H. Abdullah, A. K. Skidmore, R. Darvishzadeh, and M. Heurich, “Timing of red-edge and shortwave infrared reflectance critical for early stress detection induced by bark beetle (Ips typographus, L.) attack,” *International Journal of Applied Earth Observation and Geoinformation*, vol. 82, p. 101900, 2019.

[10] T. Klouček *et al.,* “The Use of UAV Mounted Sensors for Precise Detection of Bark Beetle Infestation,” *Remote Sensing*, vol. 11, no. 13, p. 1561, 2019.

[11] H. Abdullah, R. Darvishzadeh, A. K. Skidmore, T. A. Groen, and M. Heurich, “European spruce bark beetle (Ips typographus, L.) green attack affects foliar reflectance and biochemical properties,” *International Journal of Applied Earth Observation and Geoinformation*, vol. 64, pp. 199–209, 2018.

[12] G. A. Carter and A. K. Knapp, “Leaf optical properties in higher plants: linking spectral characteristics to stress and chlorophyll concentration,” *Am. J. Bot.*, vol. 88, no. 4, pp. 677–684, 2001.

[13] B. Wermelinger, “Ecology and management of the spruce bark beetle Ips typographus—a review of recent research,” *Forest Ecology and Management*, vol. 202, no. 1-3, pp. 67–82, 2004.

[14] T. D. Paine, K. F. Raffa, and T. C. Harrington, “Interactions among Scolytid bark beetles, their associated fungi, and live host conifers,” (eng), *Annual review of entomology*, vol. 42, pp. 179–206, 1997.

[15] B.-c. Gao, “NDWI—A normalized difference water index for remote sensing of vegetation liquid water from space,” *Remote Sensing of Environment*, vol. 58, no. 3, pp. 257–266, 1996.

[16] J. Xue and B. Su, “Significant Remote Sensing Vegetation Indices: A Review of Developments and Applications,” *Journal of Sensors*, vol. 2017, no. 1, pp. 1–17, 2017.

[17] Y. J. Kaufman *et al.,* “The MODIS 2.1- μm Channel—Correlation with Visible Reflectance for Use in Remote Sensing of Aerosol,” 35, 1286–1298., 1997.

[18] A. Karnieli, Y. J. Kaufman, L. Remer, and A. Wald, “AFRI — aerosol free vegetation index,” *Remote Sensing of Environment*, vol. 77, no. 1, pp. 10–21, 2001.

[19] P. Dutilleul, L. Nef, and D. Frigon, “Assessment of site characteristics as predictors of the vulnerability of Norway spruce (Picea abies Karst.) stands to attack by Ips typographus L. (Col., Scolytidae),” *J Appl Entomology*, vol. 124, no. 1, pp. 1–5, 2000.

[20] S. Netherer, B. Panassiti, J. Pennerstorfer, and B. Matthews, “Acute Drought Is an Important Driver of Bark Beetle Infestation in Austrian Norway Spruce Stands,” *Front. For. Glob. Change*, vol. 2, p. 265, 2019.

[21] P. Mezei, M. Potterf, J. Škvarenina, J. G. Rasmussen, and R. Jakuš, “Potential Solar Radiation as a Driver for Bark Beetle Infestation on a Landscape Scale,” *Forests*, vol. 10, no. 7, p. 604, 2019.